Supporting Information

Damschen et al. 10.1073/pnas.1308968111

SI Materials and Methods

Landscape Experiment. The orientation of each patch type around the central patch was determined by first arranging the peripheral patches so they could be contained within forest stand boundaries and then randomly selecting the direction of the corridor relative to the northern-most orientation. Prevailing wind direction was not considered. Since their creation, the patches within the experimental landscapes have been managed for open, longleaf pine savanna habitat, the dominant presettlement native vegetation type for these sites (1), by using prescribed fire and mechanical control of hardwoods and loblolly pine. The average canopy height of matrix trees is 22 m. Each landscape has a buffer area of continuous plantation forest extending >150 m from these surrounding patches' outer edges. Movement rates observed in this large-scale experiment match well (effect sizes are not significantly different) with rates of movement observed in natural landscapes at larger scales (2).

Regional Atmospheric Modeling System-Based Forest Large Eddy Simulation Model. The model surface included two replicates of each patch type separated by at least 150 m (Fig. S1), the same minimum distance between two patches in the landscape experiment. Rather than using the exact arrangement of patches in the field experiment, we chose to place each patch type on the model surface separately because this allowed us to replicate each patch type within the simulation to take an average of model runs (e.g., patches A and B in Fig. S1) and also allowed each patch type to be consistently oriented with the simulated wind direction.

Meteorological forcing consisted of a vertical profile of mean horizontal wind speed and direction, representing the regional geostrophic wind and surface fluxes. Initial conditions consisted of vertical profiles of wind (identical to the one used for forcing), pressure, temperature, and humidity, based on observations during typical warm, dry, growing season days. Monin–Obokhov similarity theory (following the formulation presented in ref. 3) was used to scale mean horizontal wind speed observations from 61 m above the ground vertically to all height levels in the simulation domain. The observed temperature and humidity were based on observations above the canopy and were scaled vertically, assuming a well-mixed boundary layer. Sensible and latent heat fluxes from the vegetation and soil were derived based on the observed 30-min mean net radiation above the canopy, light attenuation inside the canopy, and a prescribed Bowen ratio. We parameterized the sensible heat flux and Bowen ratio (in small increments around the observed values) to match the observed turbulence levels in the surface layer. The Bowen ratio, and therefore the prescribed surface fluxes, scaled with Leaf Area Index (LAI) in the forest and differed between the surrounding plantation forest and open study patches.

We quantified the physical structure of the surrounding forest matrix using the LAI from field measurements. Mean tree height of the canopy in the site was 22 m. Vertical leaf density profiles and stem taper functions were based on a pine forest in North Carolina (4). The Virtual Canopy Generator (V-CaGe, 5) was used to generate the simulated canopy. These fields include random spatial heterogeneity around the observed means of treetop height, ground-accumulated LAI, and Bowen ratio with SDs of 1.5, 0.7, and 0.23, respectively. We simulated study patches as if they were covered with grass of 0.5 LAI and 30 cm height. Bowen ratio for fluxes from the grass was slightly higher than that of tree leaves.

We plotted the mean vertical wind speed ($\overline{w}$; see color bar) as the color background of the horizontal slice figures (Fig. 2*A*; Figs. S2*A*, S3*A*, and S4*A*) because this most clearly shows the degree of persistent updrafts and downdrafts. We note that before entering a patch (i.e., far left of the figures), these wind directions may differ from above-canopy wind directions because the canopy is a porous barrier, causing the wind to gradually turn into the patch before it reaches the patch boundary and because the simulation domain has many patches close together and uses a cyclic boundary condition. However, across all of our simulation results the redirection effect consistently emerges and is strongly corroborated by the empirical wind and seed dispersal patterns (Fig. 3).

For the vertical slice figures (Figs. 2*B*; Figs. S2*B*, S3*B*, and S4*B*), we plotted the SD of vertical wind speed (σ_w) as the color background, which corresponds directly to the likelihood of uplift (see below). In addition, we directly calculated the probability of being uplifted above the canopy height (arrows in Fig. 2*B* and Figs. S2*B*, S3*B*, and S4*B*; on a log scale) relative to an equivalent height in a reference location (the center of the rectangular patch; see the red rectangle in icons to the left of the rectangular patch in Fig. 2*B* and Figs. S2*B*, S3*B*, and S4*B*). The probability of a seed located at a specific height (lower than the canopy top) to be uplifted above the canopy height given the time-averaged wind and turbulence conditions at that location can be calculated analytically using ref. 6, by substituting their equation 9 into their equation 6. The probability of uplift above the canopy, p_h, is given as

$$p_h = \frac{\exp\left(\frac{z}{h}\frac{(V_t-\overline{w})}{k\sigma_w}\right)-1}{\exp\left(\frac{(V_t-\overline{w})}{k\sigma_w}\right)-1},$$

where z is the current height of the seed, V_t is the terminal fall velocity of the seed in still air, which is positive in the downward direction (here we used $V_t = 0.7$ m/s, as was the case in the seed release experiment), $\overline{w}$ is the mean velocity of the vertical component of the wind, which is positive in the upward direction, $k = 0.41$ is the von Kármán constant, h is the mean height of the canopy top (22 m in our study system), and σ_w is turbulence in terms of the SD of the vertical wind fluctuations.

Long-Distance Dispersal Definition. There are many ways to define long-distance dispersal (LDD) events, including rarity, as determined by a proportion of seed numbers, and absolute distances (7). Because approaches based on rarity emphasize the farthest observed distances rather than a biologically meaningful distance threshold, we chose an absolute-distance definition. Absolute-distance threshold definitions can be defined using the vegetation height as a typical length scale. This can be the height of the dispersing plant, or as in the case of dispersal from an open-habitat patch in the forest, some multiples of the height of either the local vegetation in the patch or the height of the surrounding forest canopy. Other ways to define a threshold distance are based on the mean distance predicted by a simple ballistic model or the distance of a landscape barrier (e.g., the mean distance to next open-habitat patch). In our system, we chose to use the maximum dispersal distance predicted by a ballistic model (15 m) for a seed released from 4.5 m with the maximum wind speed

observed (2.2 m/s) during the seed release experiment [measured from 10 different locations at 5 and 10 m above ground layer (AGL)] as the most meaningful length scale. We note that this is not the mean dispersal distance of seeds with $V_t = 0.7$m/s, but the simplest estimate of the dispersal distance of a seed descending from (after being uplifted to) 4.5 m above the ground (and see below for an estimate of the frequency of such events). This simple approximation represents the dispersal distance based on release height, falling velocity, and wind speed alone, not accounting for vertical variation in wind speeds (updrafts–downdrafts) or the effects of habitat heterogeneity. However, our results are consistent regardless of whether we used this length (15 m) or the height of the forest canopy (22 m) as our definition of LDD threshold.

Wind Dynamics. We chose a landscape where the winged and connected patches were parallel and small-scale topography was minimized as a confounding factor. We randomly chose one of the two duplicate winged patches in which to conduct our observations. We focused on one experimental landscape because in the case of wind, it is more important to replicate the alignment of wind direction with respect to the landscape features over time rather than conducting shorter studies in multiple landscapes where the alignment of wind relative to the landscape may be inconsistent. Above-canopy wind data (from a meteorological tower ∼4 km from our experimental landscape maintained by the US Department of Energy's National Lab at the Savannah River Site, SC) were continuously collected at 15-min intervals from bivane cup anemometers at 61 m above ground. From November 2009 to January 2010, additional high-frequency data were collected using a 3D ultrasonic anemometer at the same height and these data were used to develop the atmospheric forcing conditions for the RAFLES model.

Seed Release Experiment. ***Artificial seeds.*** Artificial seeds were made out of synthetic fibers and fluorescent dye powder (DayGlo Color Corporation) and were constructed to have a terminal falling velocity (V_t) of 0.7 ± 0.025 m/s (mean ± SD), which falls well within the V_t range of native wind-dispersed plants in our study system (0.1–2.0 m/s). The unique combinations of colors for the synthetic material and fluorescent dye powder allowed identification of the release point from which a recovered seed was released.

Release events. Recent studies have reported seed release thresholds ranging from 2 to 6 m/s (8–10). We conducted five release events between October 23 and November 18, 2008 and November 27, 2009 when there was a minimum predicted wind speed aloft of 5 m/s (based on an estimation of the logarithmic wind profile from 7 y of on-site data) and winds aloft were oriented at ∼0°, 30°, and 90° relative to the long axis of the corridor. Our releases were also conducted during periods of no rain, eliminating any impact of rain on seed dispersal and detectability. Five seeds were simultaneously released every 30 s for 30 min ($n = 300$) from each release location (Table S1) in our experimental landscape. This process was repeated for five different release events, which differed in the wind direction aloft and the number of release locations used, resulting in 10 total unique combinations (Table S1) of release locations and wind direction (upwind or downwind). When there were multiple release events for one combination of release location and wind direction, the data were combined for analyses.

Seed release height. Artificial seeds were released from 4.5 m above ground to maximize our chances of observing LDD events. The specific height of 4.5 m was selected to match the height of the model's second grid layer to provide direct concordance between the model predictions and seed release experiment. Field evidence of naturally dispersing seeds confirms that 4.5 m is a biologically relevant release height. Seeds of grass and herbaceous species are released close to the ground level with a release height range of ∼0.5–3 m in our study site (11), yet a very large sample size would have been needed for seed release at that height to yield any discernible pattern of LDD because uplift is rare and the mean dispersal distance is very short (i.e., a few centimeters). Thus, the dispersal of the vast majority of seeds is not relevant to the questions addressed in this study; hence, we did not attempt to resolve the actual dispersal kernel of the local plant species. However, the relatively few seeds uplifted above the canopy, such as seeds reaching 4.5 m above the height of the understory vegetation (which is ∼0.5–4 m tall) in our study system, are very likely to disperse much farther away (12–15), hence are highly relevant to the questions addressed here. We thus chose a release height of 4.5 m to discern LDD events that are substantially more relevant to address our goal to study the general effects of patch connectivity and shape on the dispersal between patches.

Evidence from a pilot study conducted within one of our experimental landscapes provides insight into the likelihood that seeds reach 4.5 m. We captured 16,400 seeds across the dispersal season from October 2009 to January 2010 in funnel traps that were placed at 0.2, 1.5, 3.0, and 4.5 m off the ground. The proportion of total seeds captured decreased with height such that, on average, 51% ± 2.5% SE of the total seeds arrived in 0.2-m-high traps, 24% ± 1.9% SE in 1.5-m-high traps, 15% ± 1.8% SE in 3.0-m-high traps, and 10% ± 1.4% SE of seeds arrived in 4.5-m-high traps. These data confirm that far fewer seeds reach 4.5 m than lower heights, but also that an appreciable percentage of the seeds dispersing from the herbaceous understory do disperse to 4.5 m, making this release height biologically relevant.

Seed recovery. After releases were completed, seeds were recovered through systematic searches after dark using UV flashlights and their locations were recorded using a handheld geographic positioning system with submeter accuracy (Trimble Geo XT). The search area included the entire patch from which seeds were released and 25 m into the forest matrix surrounding the patches. When a seed was recovered in the matrix, a minimum additional 25 m was searched in the matrix.

Detectability. While our seed recovery rates were very high (80–100%), we also assessed our detection rate by conducting three detectability trials in both the experimental patches and in the surrounding forested matrix. We placed a known number of seeds into defined areas of matrix and patch habitat types, prevented their further movement, and had independent observers find them. The recovery rates in the matrix were 57/60, 60/60, and 180/180 (i.e., 95–100%) and in the patch were 54/60, 54/60, and 177/180 (i.e., 90–98%), suggesting that detectability was very high and did not bias our results.

Comparing Modeled and Empirical Dispersal Kernels. Because these data were not strictly independent (as the number of seeds recovered at one distance affects the number available to be recovered at other distances), we used permutation tests to determine the significance of the fit between predicted and observed data. Compared with standard parametric tests that rely on degrees of freedom to ascertain significance of the test statistic, this approach reduces problems associated with nonindependence in our significance tests. Permutation tests used 5,000 iterations, and separate regression analyses were conducted for each combination of seed release locations and events (Table S1). We performed a permutation test using the package LmPerm in R (http://cran.r-project.org/web/packages/lmPerm/index.html). To evaluate the slope from these models and determine if the slope was significantly different from 0 or 1, we generated 95% confidence limits for the slope using a bootstrap procedure based on 1,000 bootstrap replicates, implemented using the boot package in R (http://cran.r-project.org/web/packages/boot/index.html). Given the

highly stochastic turbulent processes governing seed dispersal by wind that are further complicated in fragmented landscapes like our study site, such good fits compared with other tests of mechanistic wind dispersal models suggest that RAFLES captures the underlying wind and seed dispersal processes in our study landscape and provides reasonable predictions for seed dispersal patterns.

Plant Communities. To examine the difference in species richness of wind-dispersed species among patch types, we used a mixed-model repeated-measures ANCOVA with wind-dispersed species richness as our response variable. Predictor variables included: patch type (connected, winged, rectangular) and year as fixed effects, experimental block as a random effect, and the natural log of soil moisture as a covariate because of its importance for species richness in this system (16). We modeled observations from different years as a repeated measure on the same subject (the patch) using a spatial power covariance structure, which accommodates unequal time periods between sampling events (17) due to the missing data for 2004. Degrees of freedom were adjusted by using the Kenward–Rogers method. Linear contrasts were used to determine significant differences in species richness among patch types.

Species Richness and Corridor Alignment. Wind data used in Fig. 4 are above-canopy measurements from four meteorological towers maintained by the US Department of Energy's National Lab at the Savannah River Site, SC. The towers were chosen because they were the towers closest to our experimental landscapes (located 2–8 km from our experimental blocks). Data were collected continuously at 15-min intervals from bivane cup anemometers at 61 m above ground. The wind speed and direction were averaged across the four towers and across years. Because some experimental blocks were not used for the entire 12 y, the number of years represented by the average data point in Fig. 5 ranges from 6 to 11.

1. Jose S, Jokela EJ, Miller DL eds (2006) *The Longleaf Pine Ecosystem: Ecology, Silviculture, and Restoration* (Springer, New York).
2. Gilbert-Norton L, Wilson R, Stevens JR, Beard KH (2010) A meta-analytic review of corridor effectiveness. *Conserv Biol* 24(3):660–668.
3. Nakamura R, Mahrt L (2001) Similarity theory for local and spatially averaged momentum fluxes. *Agric For Meteorol* 108(4):265–279.
4. Bohrer G (2007) Large eddy simulations of forest canopies for determination of biological dispersal by wind. PhD thesis (Duke University, Durham, NC).
5. Bohrer G, Wolosin M, Brady R, Avissar R (2007) A Virtual Canopy Generator (V-CaGe) for modeling complex heterogeneous forest canopies at high resolution. *Tellus B Chem Phys Meterol* 59B:566–576.
6. Katul GG, et al. (2005) Mechanistic analytical models for long-distance seed dispersal by wind. *Am Nat* 166(3):368–381.
7. Nathan R (2006) Long-distance dispersal of plants. *Science* 313(5788):786–788.
8. Greene DF (2005) The role of abscission in long-distance seed dispersal by the wind. *Ecology* 86(11):3105–3110.
9. Jongejans E, Pedatella NM, Shea K, Skarpaas O, Auhl R (2007) Seed release by invasive thistles: the impact of plant and environmental factors. *Proc Biol Sci* 274(1624): 2457–2464.
10. Skarpaas O, Auhl R, Shea K (2006) Environmental variability and the initiation of dispersal: Turbulence strongly increases seed release. *Proc Biol Sci* 273(1587):751–756.
11. Radford AE, Ahles HE, Bell CR (1964) *Manual of the Vascular Flora of the Carolinas* (The Univ of North Carolina Press, Chapel Hill, NC).
12. Nathan R, Katul GG (2005) Foliage shedding in deciduous forests lifts up long-distance seed dispersal by wind. *Proc Natl Acad Sci USA* 102(23):8251–8256.
13. Nathan R, et al. (2002) Mechanisms of long-distance dispersal of seeds by wind. *Nature* 418(6896):409–413.
14. Bohrer G, Katul GG, Nathan R, Walko RL, Avissar R (2008) Effects of canopy heterogeneity, seed abscission and inertia on wind-driven dispersal kernels of tree seeds. *J Ecol* 96(4): 569–580.
15. Soons MB, Heil GW, Nathan R, Katul GG (2004) Determinants of long-distance seed dispersal by wind in grasslands. *Ecology* 85(11):3056–3068.
16. Damschen EI, Haddad NM, Orrock JL, Tewksbury JJ, Levey DJ (2006) Corridors increase plant species richness at large scales. *Science* 313(5791):1284–1286.
17. Littell RC, Milliken GA, Stroup WW, Wolfinger RD (1996) *SAS System for Mixed Models* (SAS Inst., Cary, NC).

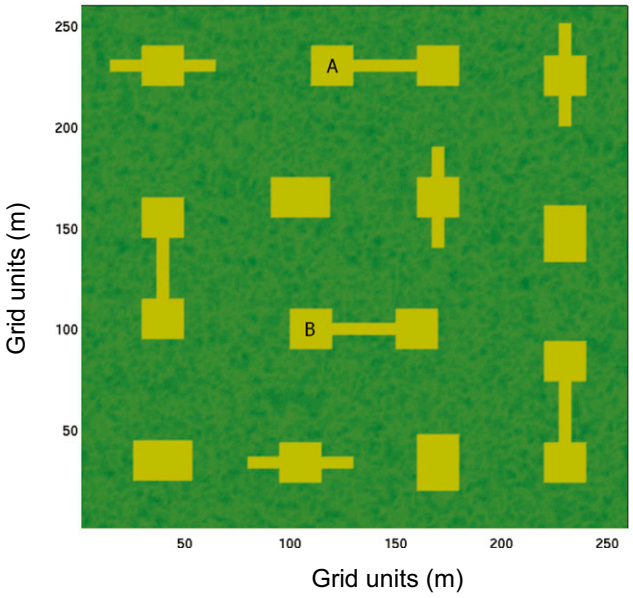

Fig. S1. Simulation domain for the RAFLES model. Two replicate patch types (e.g., A and B) were included in the simulation and results were averaged across them. Units are grid cells with 5-m resolution.

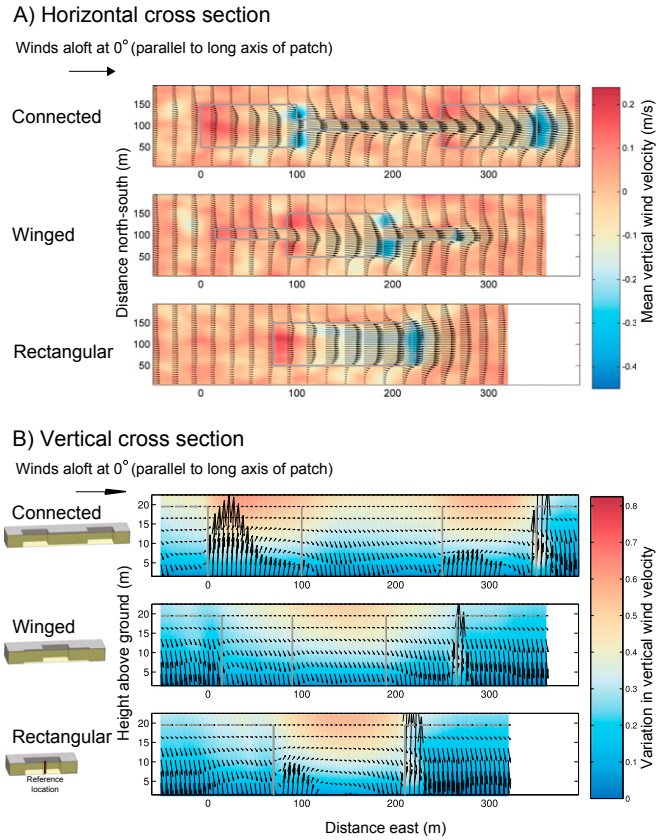

Fig. S2. Cross-sections of wind dynamics and seed ejection probabilities when overall wind forcing aloft was 0° relative to the long axis of each patch. An arrow at the top left of each panel marks the mean, above-canopy wind direction. Each figure is an average of two identical patches from different locations in the simulation domain. (*A*) Horizontal cross-section below the canopy top at 13.5 m above ground. Solid gray lines are edges of patches. The color bar shows mean vertical wind speed (red = up, blue = down). Arrows correspond to horizontal wind speeds (longer arrows indicate faster wind speeds with maximal wind speed of 2.75 m/s) and directions. (*B*) Vertical cross-section along patch centers (yellow translucent rectangle in icons to the left of each panel depicts where the vertical was taken). Solid gray lines are patch edges and dashed gray lines are the mean canopy height of 22 m. Color bar represents the SD in vertical wind velocity, where strong variation in vertical velocity (red) creates ejection hotspots. Arrows represent the uplift probability, calculated on log scale, relative to the uplift probability at the same height at a reference location at the center of the rectangular patch depicted by a red solid vertical bar in the patch icons to the left of the figure panel. Upward-pointing arrows mark locations where the probability is higher than the reference area, downward-pointing arrows where it is lower. A slight forward tilt for upward and backward tilt to downward arrows was added to make the arrows more easily distinguishable from each other.

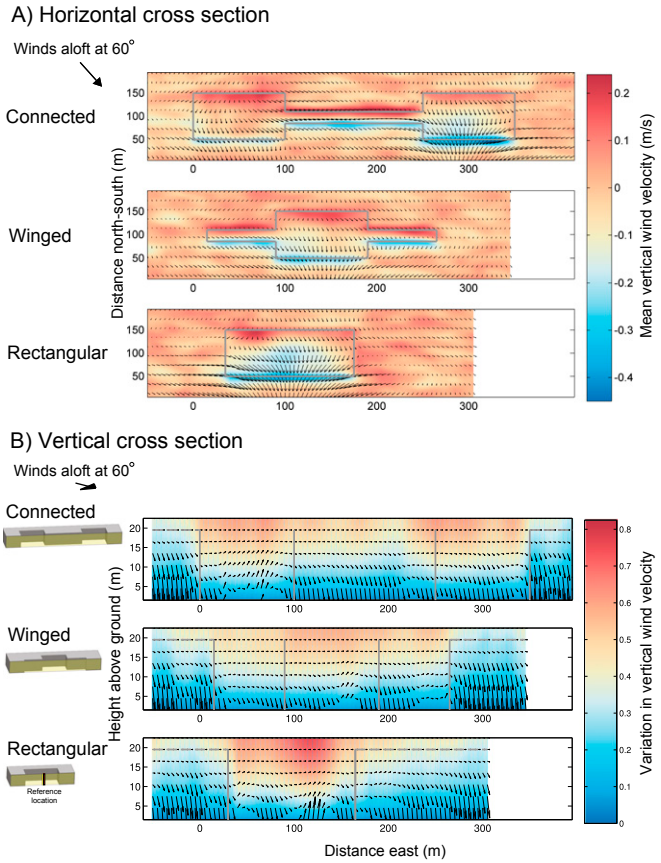

Fig. S3. Cross-sections of wind dynamics and seed ejection probabilities when overall wind forcing aloft was 60° relative to the long axis of each patch. Same as Fig. S2 but with wind oriented 60° to the long axis of the patches.

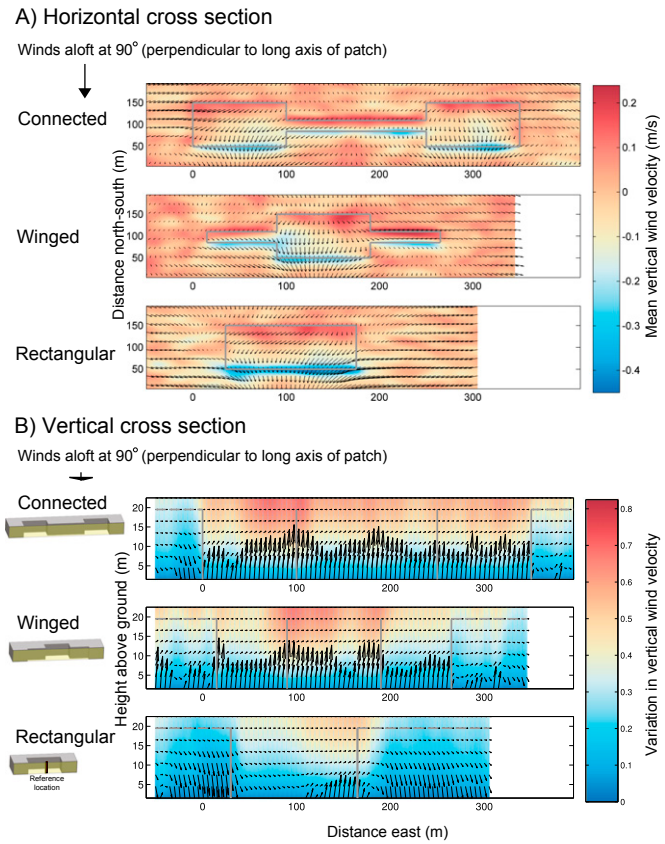

Fig. S4. Cross-sections of wind dynamics and seed ejection probabilities when overall wind forcing aloft was 90° relative to the long axis of each patch. Same as Fig. S2 but with wind oriented perpendicular (90°) to the long axis of the patches.

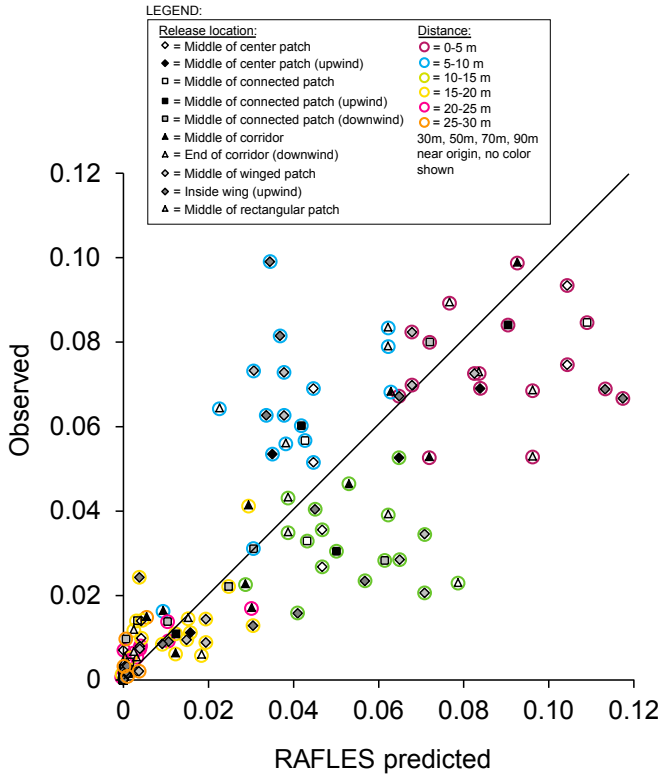

Fig. S5. Visualization of modeled (RAFLES) and observed (seed release experiments) probability densities for seeds arriving at each dispersal distance. Formal statistical comparisons were conducted for each release location separately using linear regression with permutation tests and were all significantly correlated (r^2 = 0.50–0.94; see methods above and Table S1). Each dot represents the probability of dispersing to a specific distance (colors above) from 10 different release points under different wind conditions (shapes above; Table S1). The solid black line is for reference and depicts a slope of 1. Statistical estimates of the slope were conducted for each release location separately using a bootstrap procedure and all slopes were not significantly different from 1 (see *Materials and Methods, SI Materials and Methods,* and Table S1).

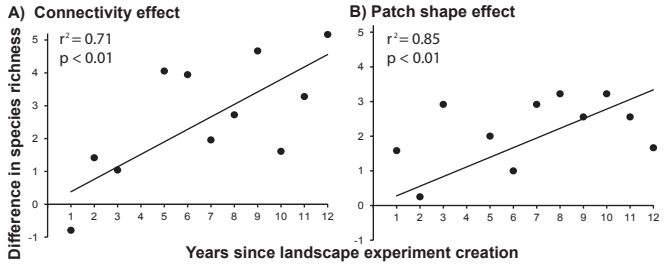

Fig. S6. Effects of (*A*) connectivity and (*B*) patch shape on wind-dispersed plant species richness over 12 y from eight experimental landscapes. Connectivity effects are the difference in species richness between connected and winged patches. Patch shape effects are the difference in species richness between winged and rectangular patches. Data through year 7 from six experimental blocks are published in ref. 1.

1. Damschen EI, et al. (2008) The movement ecology and dynamics of plant communities in fragmented landscapes. *Proc Natl Acad Sci USA* 105(49):19078–19083.

Table S1. Comparisons of modeled and observed dispersal distributions

Release	r^2	*P* value (permutation-based)	Slope (95% confidence intervals)
Middle of center patch	0.90	<0.001	0.67–1.04
Middle of center patch (upwind)	0.92	<0.001	0.78–1.50
Middle of connected patch	0.93	<0.001	0.73–3.86
Middle of connected patch (downwind)	0.81	<0.001	0.38–1.08
Middle of connected patch (upwind)	0.91	0.001	0.59–1.43
End of corridor (downwind)	0.50	0.024	0.17–1.83
Middle of corridor	0.94	<0.001	0.73–1.06
Middle of rectangular patch	0.85	<0.001	0.64–1.08
Middle of winged patch	0.64	<0.001	0.63–1.06
Inside wing (upwind)	0.57	<0.001	0.63–1.08

95% confidence limits for the slope of the relationship were generated using a bootstrap procedure. See *Methods and Materials* and *SI Materials and Methods* for a full description of the analyses used.